

## Layered double hydroxide derivatives as flame retardants for flexible PVC

Johan Labuschagné,<sup>1</sup> Dan Molefe,<sup>2</sup> Walter W Focke,<sup>\*1</sup> Osei Ofosu<sup>3</sup>

<sup>1</sup>Institute of Applied Materials, Department of Chemical Engineering, University of Pretoria, Private Bag X20, Hatfield 0028, South Africa

<sup>2</sup>Department of Chemistry, University of Pretoria, Private Bag X20, Hatfield 0028, South Africa

<sup>3</sup>CSIR Materials Science and Manufacturing, PO Box 1124, Port Elizabeth 6000, South Africa

**Summary:** The use of layered double hydroxide (LDH) derivatives as flame retardants for PVC, plasticised with 100 phr diisononyl phthalate (DINP), was investigated. Cone calorimeter results, obtained at a radiant flux of 35 kW m<sup>-2</sup>, revealed that adding 30 phr conventional magnesium-aluminium LDH lowered the peak heat release (*pHRR*) rate from 623 ± 8 kW m<sup>-2</sup> to 389 ± 9 kW m<sup>-2</sup> and reduced the smoke release by 37 %. Partial replacement of the aluminium with iron resulted in a red pigmented additive that was more effective as a flame retardant reducing the *pHRR* to as little as 253 ± 5 kW m<sup>-2</sup>. This additive also showed better smoke suppression (44 % lower) but the best smoke suppression was achieved by replacing part of the magnesium with copper (49 % lower).

**Keywords:** poly(vinyl chloride) (PVC); flame retardance; clay; smoke suppressant; plasticiser

### Introduction

PVC is a very versatile polymer used in diverse applications including flooring, rigid pipes, flexible hoses, conveyor belting, and wire- and cable-insulation. Neat PVC has a relatively high chlorine content of 56.7 wt.%, that makes it more resistant to ignition and burning than most organic polymers.<sup>[1]</sup> Furthermore, pyrolysis of PVC yields an isotropic carbon char residue <sup>[2]</sup> and this contributes to the mechanisms of flame retardant action.<sup>[3]</sup> However, the conventional plasticisers used in the manufacture of flexible PVC detract from this outstanding fire resistance. Therefore, flame-retardant (FR) and smoke-suppressant (SS) additives must be incorporated in order to meet product test specifications such as limiting oxygen index (LOI), heat release rate, smoke evolution, smoke toxicity, etc.<sup>[1]</sup> Levchik and Weil <sup>[4]</sup> and Weil *et al.*

[5] reviewed the chemical additives that have been considered to achieve acceptable fire properties in the principal PVC application areas.

Neat PVC is thermally unstable [6] and prone to autocatalytic dehydrochlorination.[7] The hydrogen chloride released assumes a catalytic role in the degradation mechanism.[8] In practice the processing problems associated with the use of PVC are overcome through the use of heat stabiliser additives.[6] Scavenging the liberated HCl generated by the degradation reaction is a way to arrest the degradation. Layered double hydroxides (LDHs) are promising heat stabilisers for PVC owing to their intrinsically high capacity to react with HCl. LDHs are anionic clays with a brucite-like structure consisting of stacks of positively charged mixed metal (Mg and Al) hydroxide layers that require the presence of interlayer anions to maintain overall charge neutrality.

Unlike most metallic salts, LDHs are readily incorporated into PVC resins to provide translucent PVC articles. The thermal stabilisation action of LDHs involves two steps. Initially HCl (formed during thermal dehydrochlorination) displaces the carbonate interlayer anions resulting in LDHs with chloride anions in the interlayer. Once this conversion is complete, the HCl will react with the clay itself, ultimately destroying its structure and forming metal chlorides, metal hydroxy-chlorides and hydrates of magnesium and aluminium.[9]

On heating LDH decomposes endothermically, releasing CO<sub>2</sub> and water vapour as inert gases. Hence it is a potential flame retardant additive for plasticised PVC as well as other polymers. In addition LDH is also a good smoke suppressant and this makes LDHs a favourable material to be used in plasticised PVC as additive to act as both heat stabiliser and flame retardant. Current industrial solutions are based on conventional MgAl-LDH. This communication considered LDH modifications related to partial or full substitution of the magnesium or aluminium constituents of conventional LDH with other metals. The effect of these modifications on the fire retardancy and smoke suppression of plasticised PVC was studied using a cone calorimeter.

## **Experimental**

**Materials.** TPC Paste Resin Co., Ltd. supplied poly(vinyl chloride) emulsion grade PG680. It was a free flowing powder with a K-value of 69. The diisononyl phthalate (DINP) plasticiser was supplied by Isegen. Al(OH)<sub>3</sub> was an industrial grade supplied by Chemical Initiatives. All other reagents used were analytical grade reagents supplied by Merck.

**Synthesis of LDH-derivatives.** The LDH-derivatives, listed in Table 1, were synthesised according to a method previously described.<sup>[10]</sup> A typical procedure for MgAl-LDH was as follows: Light MgO and Al(OH)<sub>3</sub> powders were mixed in the required 2:1 stoichiometric ratio. The powder mix was slowly added, while stirring, to one litre of distilled water in a 1.6 L Parr autoclave. A 60 mol% excess of NaHCO<sub>3</sub> was added to the mixture as the source for the intercalate anion. The final solids concentration of the slurry was 15 wt.%. The reaction was conducted under vigorous stirring at a temperature of 180 °C and a pressure of approximately 14 bar. The autoclave was kept at this temperature and pressure for approximately 5 h. Thereafter heating was discontinued and the reaction mixture was allowed to cool overnight while stirring. The solid product was removed from the autoclave, filtered and washed several times with distilled water to remove residual NaHCO<sub>3</sub> and the NaCO<sub>3</sub> byproduct. Finally it was dried in an oven at 80 °C for at least 48 h.

The substituted layered double hydroxides, i.e. LDH-derivatives, were synthesised following a similar procedure. The target was either to substitute part of the aluminium with iron(III) or part of the magnesium with copper(II) or zinc(II). For MgFeAl-LDH, 25 mol% of the Al(OH)<sub>3</sub> was substituted with Fe<sub>2</sub>O<sub>3</sub>. For MgCuAl-LDH and the MgZnAl-LDH 25 mol% of the MgO was substituted by an equivalent molar amount of the corresponding oxide. For CaAl-LDH, all of the MgO was substituted with an equal molar amount of CaO and a proprietary carbonation procedure was employed.

**Surface coating of the LDH-derivatives.** All LDH clay samples were coated with stearic acid using a procedure previously reported:<sup>[11]</sup> This was done to facilitate the homogeneous dispersion of the individual particles in the polymer matrix. The dried solids were milled into a fine powder using a coffee grinder. They were then suspended in 1 L distilled water and heated to 75 °C. The solids content of all the slurries was less than 20 wt.%. The slurries were vigorously agitated with a Silverson disperser. Stearic acid, equivalent to 2.0 wt.% based on the total dry uncoated solid sample, was added to the hot slurry. The suspension was stirred for 15 min at 6000 rpm. The coated powders were recovered by filtering. They were dried in a convection oven set at 60 °C and ground into a fine powder.

**Preparation of PVC-composites.** Diisononyl phthalate (DINP) plasticiser (130 g) was weighed into a 600 mL beaker. Next small portions of the PVC powder (up to a total of 130 g) were added and mixed-in using a high-speed mixer. The dispersion was de-aerated for about 30 min in a Speedvac vacuum chamber. Then the LDH filler powder (39 g) was incorporated. The dispersion was again de-aerated but this time for about 1 h. These plastisol samples were

used as is to test the dynamic heat stability and also to cast solid sheets for other characterisation procedures, e.g. cone calorimeter testing.

Cast PVC composite sheets were made in a three step pressing process. The paste mixture was poured into a mould measuring  $100 \times 100 \times 3.5$  mm. The mould was closed and placed in convection oven set at a temperature of  $130\text{ }^{\circ}\text{C}$  for 10 min. Then it was hot pressed at a pressure of 10 MPa at  $150\text{ }^{\circ}\text{C}$  for 5 min. The mould was then removed from the press and a heavy weight placed on the top plate. The moulding was allowed to cool down at ambient conditions before it was removed.

## **Characterisation**

**Particle size and BET surface area determination.** The particle size distributions were determined with a Malvern Instruments Mastersizer Hydrosizer 2000MY. The specific surface areas of the powders were measured with a Nova 1000e BET instrument using  $\text{N}_2$  at 77 K.

**Scanning Electron Microscopy (SEM).** A small quantity of the powdered product or the LDH precursor was placed onto carbon tape on an aluminium sample holder. Excess powder was removed using a single compressed air blast. The samples were then coated five times with carbon under argon gas using the Polaron Equipment E5200 SEM auto-coating sputter system. The powder samples were viewed on a Zeiss Ultra plus FEG SEM scanning electron microscope.

**X-ray diffraction (XRD).** X-ray diffraction analysis was performed on a PANalytical X-pert Pro powder diffractometer fitted with an X'celerator detector using Fe filtered  $\text{CoK}\alpha$  radiation ( $\lambda = 0.17901$  nm). The instrument featured variable divergence and receiving slits. X'Pert High Score Plus software was used for data manipulation and phase identification.

**Inductively coupled plasma optical emission spectrometry (ICP-OES).** The elemental composition of the LDH derivatives was determined with a Spectro Arcos inductively coupled plasma optical emission spectrometer (ICP-OES). First about 0.5 g of the clay was dissolved in 50 mL Aqua Regia. After cooling down, the reaction mixture was diluted with 50 mL of distilled water and filtered through ashless filter paper. Before performing the ICP-OES analysis, 1 mL of solution was added to 99 mL of distilled water. The analysis was then performed, analysing for copper, magnesium, aluminium, calcium, zinc, iron and sodium. The insoluble fraction was determined by ashing the filter paper.

**Mechanical Properties.** Tensile testing was carried out on a Lloyds Instruments LRX Plus machine according to the ASTM D 638 method. The crosshead speed was 50 mm min<sup>-1</sup>. Type IV dumbbells were cut from the sheets. Five specimens were tested at each composition.

**Thermogravimetric Analysis (TGA).** Thermogravimetric analysis (TGA) using the dynamic method on a Mettler Toledo A851 TGA/SDTA instrument was performed on all the samples. About 10-15 mg sample was placed in an open 150  $\mu$ L alumina pan. Temperature was scanned from 25 °C to 900 °C at a scan rate of 10 °C min<sup>-1</sup> with air or nitrogen flowing at a rate of 50 mL min<sup>-1</sup>.

**Cone calorimeter test.** The ISO 5660 standards [12-14] were followed in performing the cone calorimeter tests using a Fire Testing Technology Dual Cone Calorimeter. Three specimens of each composition were tested. The sheet dimensions were 100  $\times$  100  $\times$  3.4  $\pm$  0.1 mm. They were placed on aluminium foil and exposed horizontally to an external heat flux of 35 kW m<sup>-2</sup>. This heat flux was chosen on the basis of the study conducted by Wang *et al.* [15] They studied 3 mm to 10 mm thick PVC sheets at heat fluxes of 25 kW m<sup>-2</sup>, 35 kW m<sup>-2</sup> and 50 kW m<sup>-2</sup> and found that the time to ignition varied linearly with the inverse of the cone calorimeter heat flux. Furthermore, the minimum heat flux for ignition of sheets in this thickness range was found to be about 19 kW m<sup>-2</sup>.

**Table 1.** LDH derivatives: BET surface area, particle size and apparent elemental composition calculated from ICP-OES

Sample	Formula	BET, m <sup>2</sup> g <sup>-1</sup>	d <sub>50</sub> , $\mu$ m
MgAl-LDH	[Mg <sub>2.092</sub> Al <sub>0.908</sub> (OH) <sub>6</sub> ](CO <sub>3</sub> ) <sub>0.454</sub>	18.3	3.08 $\pm$ 0.03
CaAl-LDH	[Ca <sub>2.275</sub> Al <sub>0.725</sub> (OH) <sub>6</sub> ](OH) <sub>2</sub> CO <sub>3</sub> ) <sub>0.181</sub>	5.44	6.25 $\pm$ 0.12
MgFeAl-LDH	[Mg <sub>2.062</sub> Fe <sub>0.198</sub> Al <sub>0.740</sub> (OH) <sub>6</sub> ](CO <sub>3</sub> ) <sub>0.469</sub>	9.83	1.87 $\pm$ 0.02
MgCuAl-LDH	[Mg <sub>1.570</sub> Cu <sub>0.597</sub> Al <sub>0.833</sub> (OH) <sub>6</sub> ](CO <sub>3</sub> ) <sub>0.417</sub>	13.3	2.00 $\pm$ 0.09
MgZnAl-LDH	[Mg <sub>1.527</sub> Zn <sub>0.554</sub> Al <sub>0.918</sub> (OH) <sub>6</sub> ](CO <sub>3</sub> ) <sub>0.458</sub>	12.4	2.30 $\pm$ 0.11

## Results

Table 1 reports the ICP-OES chemical composition results in terms of the general formula: [Mg<sub>2+ $\alpha$</sub> Al<sub>1- $\alpha$</sub> (OH)<sub>6</sub>](CO<sub>3</sub>)<sub>(1- $\alpha$ )/2</sub>·xH<sub>2</sub>O. The apparent  $\alpha$  value varied from 0.08 (MgZnAl-LDH) to 0.28 (CaAl-LDH). It also reports the d<sub>50</sub> particle sizes and the BET specific surface areas for

the LDH-derivatives. The median ( $d_{50}$ ) particle size varied from 1.9  $\mu\text{m}$  to 6.25  $\mu\text{m}$ . BET surface was highest for MgAl-LDH (18.3  $\text{m}^2 \text{g}^{-1}$ ) and lowest for CaAl-LDH (5.44  $\text{m}^2 \text{g}^{-1}$ ).

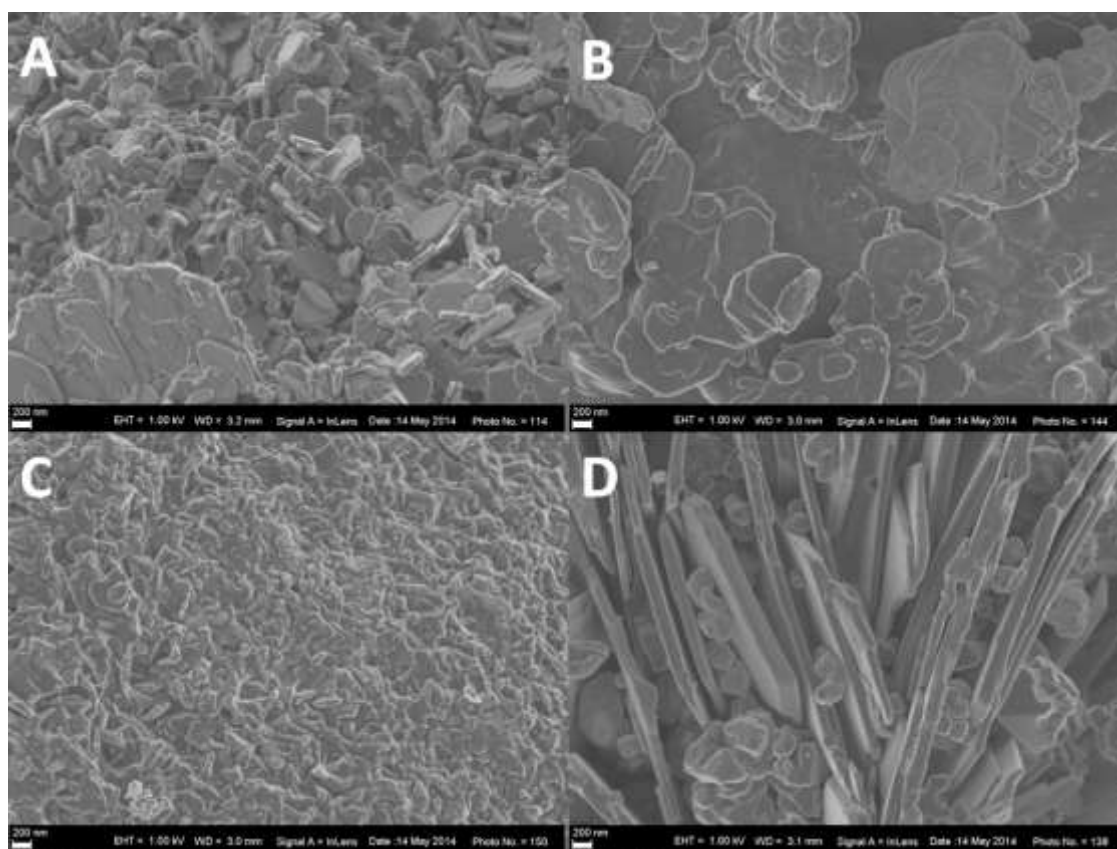


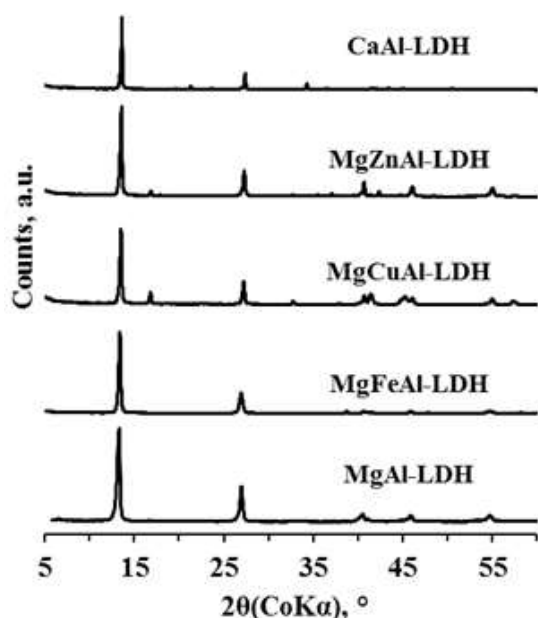
**Figure 1.** SEM micrographs of (A) MgZnAl-LDH; (B) MgFeAl-LDH; (C) MgCuAl-LDH, and (D) CaAl-LDH. The size bar indicates a length of 200 nm.

**Table 2.** LDH derivatives: TGA residue at 900 °C and d-spacing from XRD results.

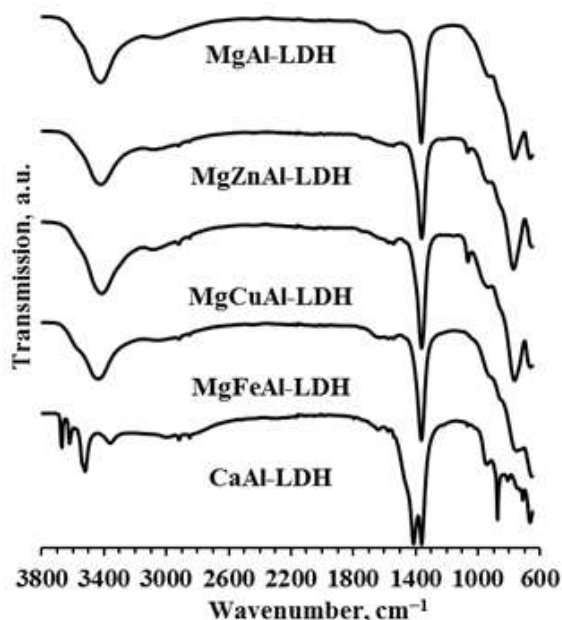
Sample	Residue, %	d-spacing, nm
MgAl-LDH	57.0	0.761
MgCuAl-LDH	65.6	0.761
MgZnAl-LDH	61.9	0.758
MgFeAl-LDH	56.3	0.768
CaAl-LDH	59.2	0.755

Figure 1 shows FEG SEM micrographs of some LDH-derivative powders. The individual powder particles are made up of highly agglomerated flake-shaped crystals. The primary flakes were smallest for MgCuAl-LDH and largest for CaAl-LDH. The micrograph for the latter actually shows an edge-on view whereas the other micrographs show a top view. The XRD patterns shown in Figure 2 feature reflections characteristic of LDHs.<sup>[16]</sup> The reflections at  $2\theta = 13.474^\circ$  and  $2\theta = 27.125^\circ$  in the XRD diffractogram for MgAl-LDH are consistent with a

brucite layer basal spacing of 0.761 nm. The d-spacing values for the other compounds are listed in Table 2. It was slightly larger (0.768 nm) for the MgFeAl-LDH and slightly lower (0.755 nm) for CaAl-LDH than the value for MgAl-LDH (0.761 nm) but consistent with literature reports.<sup>[17-19]</sup> The sharp nature of the reflections points to a high crystallinity of the corresponding powders.



**Figure 2.** X-ray diffraction patterns for the various LDH derivatives



**Figure 3.** FTIR spectra of the various LDH derivatives

Figure 3 shows that all the FTIR spectra, except the one for CaAl-LDH, were very similar. The presence of the stearic acid coating is evident from the two small peaks observed between  $2993\text{ cm}^{-1}$  and  $2961\text{ cm}^{-1}$  for CaAl-LDH, MgZnAl-LDH, MgCuAl-LDH and MgFeAl-LDH respectively. The broad band that is observed at ca.  $3470\text{ cm}^{-1}$  is attributed to  $\text{-OH}$  stretching vibrations in the octahedral layer and the free and hydrogen bonded water molecules present in the interlayer. The strong sharp peaks near  $1366\text{ cm}^{-1}$  are due to the  $\text{CO}_3^{2-}$   $\nu_3$  antisymmetric vibrations. The CaAl-LDH shows two strong peaks here, suggesting the presence of two different environments for carbonate ions. The compound synthesised was actually calcium hemicarboaluminate ( $[\text{Ca}_4\text{Al}_2(\text{OH})_{12}] \text{OH}(\text{CO}_3)_{0.5} \cdot 4\text{H}_2\text{O}$ ). In this clay half the interlayer carbonate ions are substituted by hydroxyl ions.

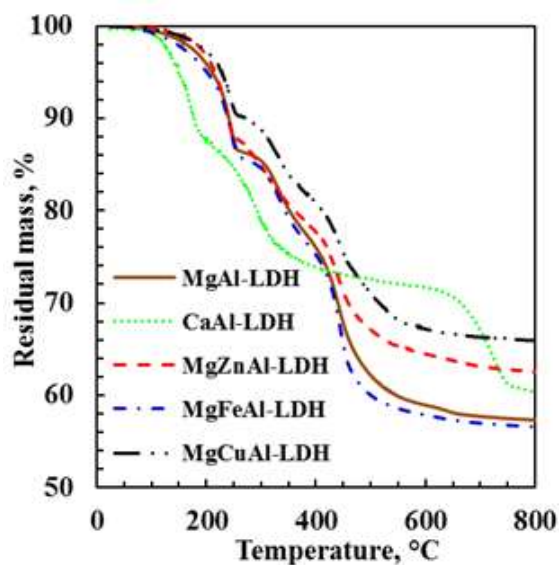


**Figure 4.** TGA traces in air for the LDH derivatives. Temperature was scanned from 25 °C to 900 °C at a scan rate of 10 °C min<sup>-1</sup> with air flowing at a rate of 50 mL min<sup>-1</sup>.

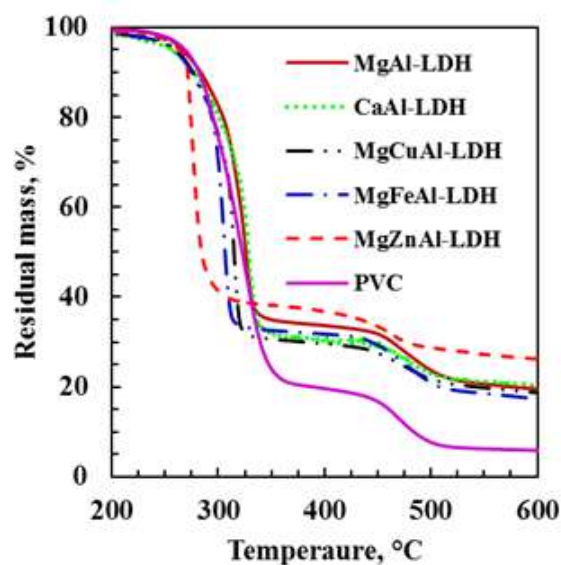


**Figure 5.** TGA traces in N<sub>2</sub> for the PVC-LDH composites. Temperature was scanned from 25 °C to 900 °C at a scan rate of 10 °C min<sup>-1</sup> with nitrogen flowing at a rate of 50 mL min<sup>-1</sup>.

Figure 4 summarises the TGA mass loss curves for various LDH samples as obtained in an air atmosphere. All the derivatives showed the three distinct mass loss steps expected for LDH during thermal decomposition.<sup>[20, 21]</sup> They correspond to dehydration, dehydroxylation and finally the removal of the interlayer carbonate anion. The first step is usually the loss of physisorbed and interlayer water, which commences at about 50 °C and is complete by 150 °C.<sup>[22]</sup> Mass loss commenced earlier and was initially more pronounced for CaAl-LDH. It lost about 12 wt.% mass by 190 °C. However, between 460 °C and 700 °C the cumulative mass loss was less than that found for the other LDH derivatives. Above the latter temperature, CaAl-LDH showed mass loss behaviour reminiscent of that expected for calcium carbonate. CaAl-LDH showed a total mass loss of 41 wt.% at 900 °C. The initial mass loss for MgAl-LDH, MgZnAl-LDH, MgCuAl-LDH and MgFeAl-LDH were quite similar. However, compared to the other compounds, the TGA mass loss curve of MgCuAl-LDH appeared shifted to higher temperatures. The first mass loss event commenced at around 130 °C and was complete by about 250 °C showing a mass loss of ca. 12 wt.%. The second mass loss event is more or less complete by 350 °C at which point the mass loss had reached about 30 wt.%. Mass loss was effectively complete by about 700 °C. The residues, recorded at 900 °C, are listed in Table 2.



**TGA of the LDH-PVC composites.** The thermogravimetric analysis on PVC compounds provides basic information on the intrinsic heat stability of the PVC compounds. Figure 5 shows TGA traces for the LDH-PVC compounds recorded in a nitrogen atmosphere. The flexible PVC apparently suffers two major mass loss stages. The first commences at 240 °C, reaches a maximum rate at 315 °C and ends at 370 °C. At this point the residue is 20.7 wt.%. The second stage starts as 420 °C, reaches a maximum rate at 467 °C and ends at 510 °C with a residue of 7.0 wt.% remaining. However, the derivative curves (DTG not shown) show multiple peaks in the mass loss stage. The initial mass losses are due a combination of PVC degradation (mainly dehydrochlorination) events and volatilisation of the plasticiser. The second stage is attributed to pyrolysis reactions that ultimately lead to a carbonaceous char residue (4.3 wt.% at 900 °C). The shape of the mass loss curves for the LDH-PVC composites mirror those of PVC. The mass loss onset temperatures are virtually identical but mass loss occurs over a narrower temperature range. The residue after each stage is greater than found for the neat PVC. The ranking for initial mass loss rate, from fastest to slowest, for the additives at peak decomposition is:

MgZnAl-LDH >> MgFeAl-LDH > MgCuAl-LDH > CaAl-LDH ≈ MgAl-LDH

The MgZnAl-LDH, in particular, significantly accelerated the mass loss during the first stage. The initial decomposition yields ZnCl<sub>2</sub> which autocatalytically accelerates the dehydrochlorination reaction according to the mechanism reported by Levchik and Weil.<sup>[4]</sup> This is also known as zinc poisoning in industry. The higher char yield is also attributed to catalytic effects that favour crosslinking and aromatisation reactions at the expense of cracking reactions that yield volatiles.



**Figure 6.** Physical appearance of the pressed PVC sheets

**Physical appearance of the LDH-PVC composites.** Figure 6 shows colour images of the moulded sheets. The discoloration of the PVC sample is attributed to the fact that no stabiliser was used at all. Strong pigmenting effects were observed with the MgFeAl-LDH (red) and the MgCuAl-LDH (black) additives.

**Table 3.** Mechanical properties (tensile strength, Young's modulus and elongation to break) of the PVC compounds filled with the LDH derivatives

Sample	$\sigma$ , MPa	E, MPa	$\varepsilon$ , %
PVC	$4.16 \pm 0.13$	$2.8 \pm 0.3$	$250 \pm 7$
MgAl-LDH	$4.46 \pm 0.09$	$3.3 \pm 0.2$	$316 \pm 7$
CaAl-LDH	$2.82 \pm 0.14$	$2.4 \pm 0.2$	$226 \pm 11$
MgFeAl-LDH	$4.28 \pm 0.12$	$2.7 \pm 0.2$	$316 \pm 11$
MgCuAl-LDH	$3.55 \pm 0.26$	$3.0 \pm 0.2$	$222 \pm 25$
MgZnAl-LDH	$3.73 \pm 0.18$	$3.3 \pm 0.5$	$262 \pm 22$

**Table 4.** Cone calorimeter data summary

Parameter	Units	PVC	MgAl LDH	CaAl LDH
Time to ignition ( $t_{ign}$ )	s	$23.0 \pm 2.1$	$27.7 \pm 1.2$	$18.0 \pm 0.1$
Time to flame out	s	$306 \pm 137$	$654 \pm 51$	$442 \pm 21$
Time to $pHRR$	s	$103 \pm 10$	$105 \pm 1$	$145 \pm 9$
$pHRR$	$\text{kW m}^{-2}$	$623 \pm 8$	$389 \pm 9$	$381 \pm 24$
Total heat release ( $tHR$ )	$\text{MJ m}^{-2}$	$68 \pm 2$	$72 \pm 3$	$78 \pm 3$
FIGRA	$\text{kW m}^{-2}\text{s}^{-1}$	$6.1 \pm 0.6$	$3.7 \pm 0.1$	$2.6 \pm 0.2$
MAHRE	$\text{kW m}^{-2}$	$367 \pm 11$	$208 \pm 2.2$	$241 \pm 13.1$
FPI ( $t_{ign}/pHRR$ )	$\text{s m}^2\text{kW}^{-1}$	$0.037 \pm 0.004$	$0.072 \pm 0.001$	$0.047 \pm 0.003$
Smoke release	$\text{m}^2 \text{m}^{-2}$	$4413 \pm 97$	$2780 \pm 121$	$3153 \pm 292$
		MgFeAl LDH	MgCuAl LDH	MgZnAl LDH
Time to ignition ( $t_{ign}$ )	s	$24.0 \pm 1.0$	$21.7 \pm 1.5$	$23.7 \pm 0.6$
Time to flame out	s	$649 \pm 41$	$482 \pm 56$	$638 \pm 27$
Time to $pHRR$	s	$45 \pm 0$	$107 \pm 3$	$40 \pm 0$
$pHRR$	$\text{kW m}^{-2}$	$253 \pm 5$	$383 \pm 22$	$319 \pm 7$
Total heat release ( $tHR$ )	$\text{MJ m}^{-2}$	$72 \pm 3$	$64 \pm 4$	$74 \pm 7$
FIGRA	$\text{kW m}^{-2}\text{s}^{-1}$	$5.6 \pm 0.1$	$3.7 \pm 0.3$	$8.0 \pm 0.2$
MAHRE	$\text{kW m}^{-2}$	$176 \pm 1.3$	$208 \pm 7.5$	$195 \pm 3.3$
FPI ( $t_{ign}/pHRR$ )	$\text{s m}^2\text{kW}^{-1}$	$0.095 \pm 0.003$	$0.056 \pm 0.007$	$0.074 \pm 0.001$
Smoke release	$\text{m}^2 \text{m}^{-2}$	$2468 \pm 15$	$2244 \pm 216$	$2971 \pm 136$

$pHRR$ : Peak heat release rate

**Mechanical properties of the LDH-PVC composites.** Table 3 shows the effect of the additives on the tensile properties of plasticised PVC. A marginal reinforcing effect was observed for MgAl-LDH and MgZnAl-LDH but the stiffness of the sample containing CaAl-LDH was actually lower than that of the neat PVC compound. The latter sample also showed

a reduced tensile strength although the elongation to break was in the range of those observed for the other compounds. The poor performance of this sample is not currently understood but could be related to the large particle size of this additive compared to the others. Otherwise the mechanical properties were similar to those for the base PVC compound.

**Flammability.** The cone calorimeter results are presented in Figure 7 and Figure 8 and they are summarised in Table 4. All the samples ignited after a short but similar induction period. They burned producing a large amount of smoke. For purposes of readability and clarity, some of the figures show only the data obtained for the neat PVC, the compound containing the reference additive MgAl-LDH and the compound that provided the best performance in each category. The time to ignition ( $t_{ign}$ ) was  $23 \pm 2$  s for the neat PVC compound. It was longest for the MgAl-LDH containing compound ( $28 \pm 1$  s) and shortest for CaAl-LDH ( $18 \pm 0$  s). The time to flame out was  $306 \pm 137$  s for the neat PVC compound. It increased by between 44% and 112% with LDH added.

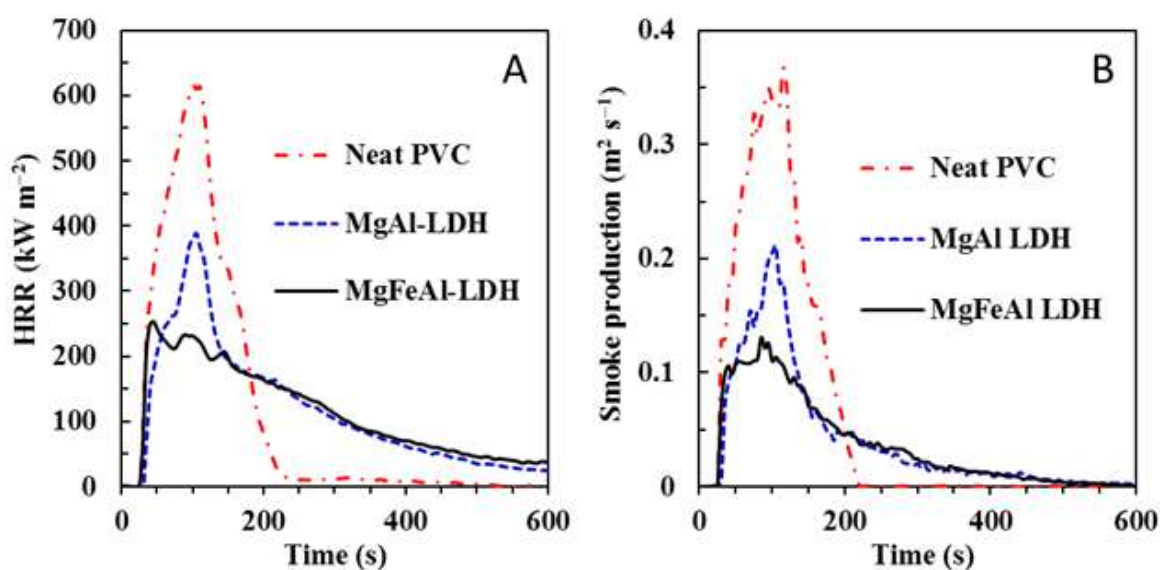


**Figure 7.** (A) Representative cone calorimeter heat release rate curves, and (B) smoke production rates for the plasticised PVC compound and its composites with LDH derivatives. The sample sheets were backed by aluminium foil and their dimensions were 100 mm × 100 mm × 3.5 ± 0.1 mm. They were exposed horizontally to an external heat flux of 35 kW m<sup>-2</sup>.

Directly after ignition, the neat PVC compound showed rapid mass loss and this was virtually complete by 200 s. Thereafter there was a very slow steady decline in the residue amount with the char yield in the order of 3 wt.% at the end of the test. The LDH composites lost mass at a much slower rate over a longer time. Up to about 150 s into the test, the mass loss curves

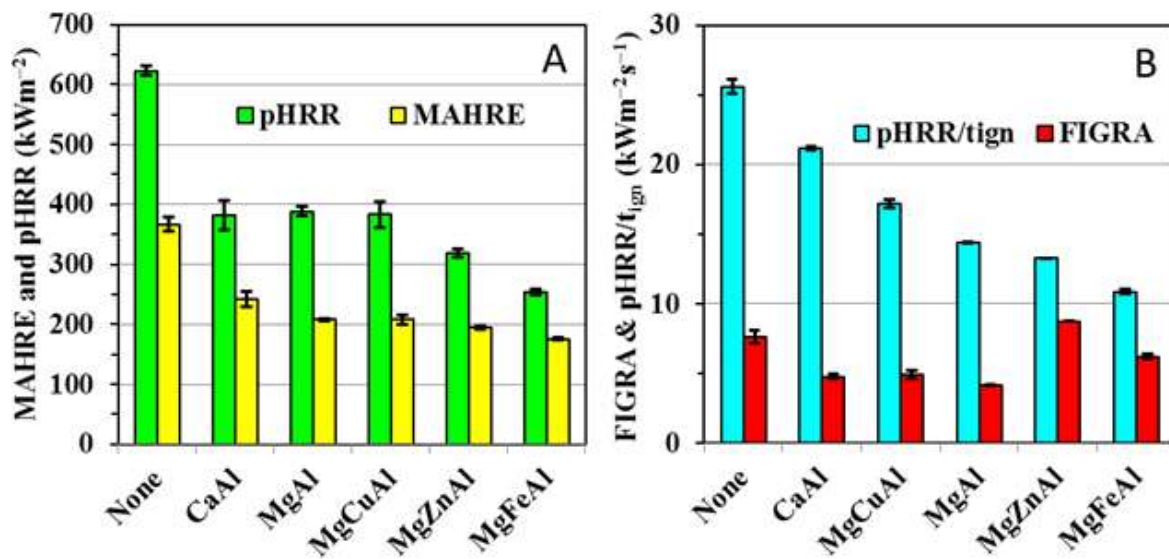
virtually coincided. After this time they diverged with CaAl-LDH showing the greatest mass loss and MgZnAl-LDH the least. These compounds spanned the char yields of the others with ca. 13 wt.% and 20 wt.% respectively. The faster initial mass loss and the higher ultimate char yield found for the MgZnAl-LDH agrees with behaviour observed in the TGA pyrolysis run in a nitrogen atmosphere.

Figure 7 shows representative heat release rate (*HRR*) and smoke production curves obtained from the cone calorimeter tests. The heat release curves for the neat plasticised PVC compound exhibited the shape approaching the characteristic of a thermally thin sample.<sup>[23]</sup> Thermally thin samples are identified by a sharp peak in their *HRR* curves as the whole sample is pyrolysed nearly at once. The *HRR* curves for the filled compounds were flatter and broader than that for the neat PVC. *HRR* curves characteristic of thermally thick, char-producing samples show a sudden rise to a plateau value.<sup>[23]</sup> However, the *HRR* curves for the samples containing LDH derivatives were more complex. They showed a sudden rise to a peak value with a slow but steady decline over a longer time period. The CO<sub>2</sub> and CO release rates (not shown graphically) curves mirrored those observed for the *HRR* (Figure 5) almost perfectly. Figure 7 (B) shows representative smoke production rates (*SPR*) and Table 3 compares the smoke production of the composites with that for the neat PVC compound. The LDH derivatives composites featured lower *SPR* in comparison to the neat PVC just as they also featured reduced rates of mass loss under flaming conditions. The lowest peak value was observed with MgFeAl-LDH (Figure 7 (B)) but the lowest overall smoke release was obtained with MgCuAl-LDH as shown in Table 3.

Figure 8A shows the effect of adding the LDH fillers to the PVC on the peak heat release rates (*pHRR*) and the maximum average rate of heat emission (*MAHRE*). The *pHRR* for the neat PVC compound was  $623 \pm 8 \text{ kW m}^{-2}$ . Incorporating LDH derivatives at the 13 wt.% level caused a significant lowering of the *pHRR*. MgAl-LDH lowered the *pHRR* value to  $389 \pm 9 \text{ kW m}^{-2}$  but the best result was obtained with MgFeAl-LDH ( $253 \pm 5 \text{ kW m}^{-2}$ ).

An important index used to interpret cone calorimeter data is the maximum average rate of heat emission (*MAHRE*).<sup>[23, 24]</sup> The *MAHRE* parameter is defined as the peak value of the cumulative heat emission divided by time.<sup>[24]</sup> It provides a measure of the propensity for fire development under full scale conditions. The addition of the LDH derivatives significantly reduced the *MAHRE*. On the whole the reduction follows the same trend that was observed for the peak heat release rate. The *MAHRE* for the neat PVC was  $367 \pm 11 \text{ kW m}^{-2}$  and this was reduced to  $176 \pm 1 \text{ kW m}^{-2}$  with the MgFeAl-LDH as stabiliser-flame retardant.

Interesting observations hold for the total heat release ( $tHR$ ). It was  $68 \pm 2 \text{ MJ m}^{-2}$  for the neat PVC compound (Table 3). With the LDH derivatives incorporated, the  $tHR$  increased even though less fuel is actually available. The  $pHRR$  was  $72 \pm 3 \text{ MJ m}^{-2}$  for the MgAl-LDH compound and the highest value was  $78 \pm 3 \text{ MJ m}^{-2}$  recorded for the CaAl-LDH. Thus while the fire performance improved with respect to the peak heat release rate, it deteriorated when the total heat release is considered. The apparent increase in the total heat release ( $tHR$ ) is tentatively attributed to the chlorine preferentially interacting and bonding with the LDH. This means that more of the carbon became available as fuel.



**Figure 8.** The effect of the LDH derivatives on (A) the cone calorimeter peak heat release rates and  $MAHRE$ , and (B) the  $FIGRA$  and  $pHRR/t_{ign}$  of PVC composites. The sample sheets were backed by aluminium foil and their dimensions were  $100 \text{ mm} \times 100 \text{ mm} \times 3.5 \pm 0.1 \text{ mm}$ . They were exposed horizontally to an external heat flux of  $35 \text{ kW m}^{-2}$ .

The fire growth rate ( $FIGRA$ ) is an estimator for the fire spread rate and size of the fire.<sup>[23, 24]</sup> Strictly speaking the  $FIGRA$  is defined as the maximum quotient of  $HRR(t)/t$ . The fire performance index (FPI) is possibly the best single indicator of the overall fire hazard posed by a material.<sup>[25]</sup> It is defined as the ratio of the time-to-ignition to the peak heat release rate ( $FPI = t_{ign}/pHRR$ ). There is a connection between  $FPI$  and the time to flashover, i.e. the change from small to large-scale fire:<sup>[25]</sup> A lower  $FPI$  value is associated with a shorter time to flashover suggesting that a shorter time is available for escape in a full-scale fire situation. Figure 7 shows the  $FIGRA$  and  $FPI$  indices with the latter expressed as its inverse as it then has the same units as the  $FIGRA$ . Relative to the neat PVC compound, the presence of the MgAl-LDH or the CaAl-LDH markedly decreased the  $FIGRA$  (>50%). However, a significant higher

value was found for the MgZnAl-LDH. The  $pHRR/t_{ign}$  for the neat PVC was  $26 \pm 1 \text{ kW m}^{-2} \text{ s}^{-1}$ . It was lowered to  $10.9 \pm 0.2 \text{ kW m}^{-2} \text{ s}^{-1}$  in the presence of MgFeAl-LDH while the other PVC compounds featured intermediate values.

## Discussion

Compared to the neat PVC, the LDH-stabilised PVC samples showed different behaviour in the TGA and cone calorimeter tests. There was also a clear LDH composition effect. The MgZnAl-LDH accelerated the initial TGA mass loss in a nitrogen atmosphere but led to relatively high char yields at higher temperatures. In the cone calorimeter tests, they generally decreased the time to ignition and increased the time to flame out. They also increased the total fire load, but proved to be effective flame retardants with respect to all other fire performance indices. MgFeAl-LDH was most effective at reducing the peak heat release rate ( $pHRR$ ), the maximum average rate of heat emission ( $MAHRE$ ) and increasing the fire performance index ( $FPI$ ). MgAl-LDH led to the lowest fire growth rate ( $FIGRA$ ) while MgCuAl-LDH showed the lowest smoke production.

The performance of the LDH-derivatives can be explained in the context of the PVC degradation mechanism. Neat PVC degradation occurs in two stages. The first stage proceeds as an autocatalytic dehydrochlorination of the PVC backbone with the liberated hydrogen chloride assuming a catalytic role.<sup>[8]</sup> The degradation reaction is initiated at defect sites (e.g., internal allylic chloride and tertiary chloride structural flaws). The mechanism of autocatalysis involves a free-radical process that converts ordinary polymer repeat units into chloro-allylic structures of low thermal stability.<sup>[7]</sup> It also leads to the formation of sequences of conjugated double bonds along the polymer chain. In the second stage of degradation these highly reactive defects undergo secondary reactions. Crosslinking of the polymer chains and dehydrocarbonation reactions promote char formation.<sup>[26]</sup> Chain cleavage and cracking reactions led to the formation of volatile aromatic molecules that promote smoke generation.

The hydrochloric acid generated by the degradation reaction catalyses the chain propagation reaction. The carbonated LDHs improve the heat stability of the PVC by scavenging this corrosive gas.<sup>[3]</sup> Initially this occurs via the formation of chloride intercalated LDHs. However, later on the acid attacks the LDH structure leading to the formation of metal chlorides. These salts act as Lewis bases that can also promote dehydrochlorination via a carbonium ion mechanism.<sup>[4]</sup>  $\text{ZnCl}_2$  in particular appears to be a more active catalyst than HCl. This explains

the faster mass loss observed for the MgZnAl-LDH compound during the initial stages of the degradation and recorded in both the cone calorimeter and in the TGA experiments.

According to Zhu *et al.* [27] the LDHs act as Lewis acids and induce cationic crosslinking (Friedel–Craft reaction) of neighbouring polyene backbones. Metal chlorides also catalytically favour crosslinking and dehydrocarbonation reactions at the expense of cracking reactions.[27] These actions improve char formation and reduce smoke generation in accordance with the present experimental results. Copper ions acts as reductive crosslinking agent and this may explain the observation that the MgCuAl-LDH compound was a particularly effective smoke suppressant.

The release of the HCl by the decomposing PVC inhibits flaming combustion in the cone calorimeter tests. The halogen entering the gas phase contributes to a “flame poisoning effect”, i.e. the slowing down of the free radical chain reactions occurring in the flame.[5] In the presence of the LDHs, the HCl is efficiently scavenged especially in the early stages of degradation. Less halogen is present in the volatile organics released in the beginning, making them easier to ignite. This may explain the shorter time to ignition found for some LDH compounds compared to neat PVC.

Compared to the neat PVC, all the LDH compounds decreased the peak heat release rate in the cone calorimeter tests. This may be due to a combination of vapour phase and solid phase effects. High heat decomposes the LDHs, releasing water and carbon dioxide. The decomposition is endothermic in nature which means that it cools the polymer substrate. At lower temperature the degradation reactions that generate fuel proceeds more slowly. This explains, in part, the lower rate of mass loss observed for the LDH compounds in the cone calorimeter tests. In addition, the inert gases liberated have a dilution effect on the air-fuel mixture in the gas phase. This cools the flame and reduces the rate of heat generation. The inorganic residues may also form a protective layer on the surface of the substrate. They may act as a barrier to heat transfer to the underlying polymer and also as a barrier to mass transfer of degradation products migrating to the gas phase. Finally the inorganic residues may effectively reflect incoming infrared radiation that would otherwise have heated the substrate to higher temperatures. All these effects may contribute to the lowering of the heat release rate observed in the cone calorimeter tests. Finally, at elevated temperature and in the presence of oxygen, the metal oxide residues from the decomposition of the LDHs catalyse the oxidation of the carbonaceous char residues.

## Conclusions

Emulsion grade PVC was plasticised with 100 phr of diisononyl phthalate (DINP) and filled with 30 phr layered double hydroxides (LDHs) as combination stabiliser-flame retardant. The MgAl-LDH with approximate composition  $[\text{Mg}_4\text{Al}_2(\text{OH})_{12}](\text{CO}_3)\cdot 3\text{H}_2\text{O}$  was chosen as reference additive. Derivatives in with partial substitution of the magnesium or the aluminium with zinc, copper, iron or full substitution with calcium were also evaluated. The thermal decomposition was studied by thermogravimetric analysis and the fire behaviour determined in a cone calorimeter. The addition of LDH derivatives significantly improved the fire resistance of the plasticised PVC. Partial substitution of the aluminium by Fe(III) in the LDH lowered the peak heat release rate (*pHRR*), from  $623 \pm 8 \text{ kW m}^{-2}$  to  $253 \pm 5 \text{ kW m}^{-2}$  but increased the total heat release from  $68 \pm 2 \text{ MJ m}^{-2}$  to  $72 \pm 3 \text{ MJ m}^{-2}$ . This MgFeAl-LDH also improved other fire resistance indices, e.g. the maximum average rate of heat emission (*MAHRE*) and the fire performance index (*FPI*). MgAl-LDH showed the lowest fire growth rate (*FIGRA*) while the MgCuAl-LDH showed the lowest smoke production.

## Acknowledgements

Financial support from the *THRIP* programme of the Department of Trade and Industry and the National Research Foundation as well as Greenfield Innovation, Engelbrecht & Mentz and Blue Sky Venture Partners is gratefully acknowledged.

## References

- [1] A. W. Coaker, *J. Vinyl Addit. Technol.* **2003**, 9, 108.
- [2] S. Otani, *Carbon* **1965**, 3, 31.
- [3] O. M. Folarin, E. R. Sadiku, *Int. J. Phys. Sci.* **2011**, 6, 4323.
- [4] S. V. Levchik, E. D. Weil, *Polym. Adv. Technol.* **2005**, 16, 707.
- [5] E. D. Weil, S. Levchik, P. Moy, *J. Fire Sci.* **2006**, 24, 211.
- [6] D. Braun, *J. Polym. Sci., Part A: Polym. Chem.* **2004**, 42, 578.
- [7] W. H. Starnes Jr, X. Ge, *Macromolecules* **2004**, 37, 352.
- [8] W. H. Starnes Jr, *Prog. Polym. Sci. (Oxford)* **2002**, 27, 2133.
- [9] L. van der Ven, M. L. M. van Gemert, L. F. Batenburg, J. J. Keern, L. H. Gielgens, T. P. M. Koster, H. R. Fischer, *Appl. Clay Sci.* **2000**, 17, 25.
- [10] F. J. W. J. Labuschagné, E.W.Giesekke, J. D. Van Schalkwyk. Production of Hydrotalcite. South African Patent 9947, 2007.
- [11] F. J. W. J. Labuschagne, D. M. Molefe, W. W. Focke, I. Van Der Westhuizen, H. C. Wright, M. D. Royeppen, *Polym. Degrad. Stab.* **2015**, 113, 46.
- [12] ISO 5660-1: 2002 Reaction to fire tests. Heat release, smoke production and mass loss rate, *Part 1: Heat release rate (cone calorimeter method) and smoke production rate (dynamic measurement)*, ISO, Geneva, Switzerland, 2002.



- [13] ISO 5660-2: 2002. Reaction to Fire Tests. Heat Release, Smoke Production and Mass Loss Rate, *Part 2: Smoke Production Rate (Dynamic Measurements)*, ISO, Geneva, Switzerland, 2002.
- [14] ISO/TR 5660-3: 2003. Reaction to Fire Tests. Heat Release, Smoke Production and Mass Loss Rate, in *Part 3: Guidance on Measurement*, ISO, Geneva, Switzerland, 2003.
- [15] Z. Wang, Huang, P., Fan, W.C., Wang, Q., "Measurements on the fire behaviour of PVC sheets using the cone calorimeter", in *Proceedings of the Asia-Oceania Symposium on Fire Science & Technology*, International Association for Fire Safety Science, 1988, p. AOFST 3/221.
- [16] F. Cavani, F. Trifirò, A. Vaccari, *Catal. Today* **1991**, *11*, 173.
- [17] M. François, G. Renaudin, O. Evrard, *Acta Crystallogr., Sect. C: Cryst. Struct. Commun.* **1998**, *54*, 1214.
- [18] G. Renaudin, M. Francois, O. Evrard, *Cem. Concr. Res.* **1999**, *29*, 63.
- [19] T. Runčevski, R. E. Dinnebier, O. V. Magdysyuk, H. Pöllmann, *Acta Crystallogr., Sect. B: Struct. Sci.* **2012**, *68*, 493.
- [20] W. T. Reichle, *J. Catal.* **1985**, *94*, 547.
- [21] L. Moyo, W. W. Focke, D. Heidenreich, F. Labuschagne, H.-J. Radusch, *Mater. Res. Bull.* **2013**, *48*, 1218.
- [22] R. L. Frost, W. Martens, Z. Ding, J. T. Klopogge, *J. Therm. Anal. Calorim.* **2003**, *71*, 429.
- [23] B. Schartel, T. R. Hull, *Fire Mater.* **2007**, *31*, 327.
- [24] M. Sacristán, T. R. Hull, A. A. Stec, J. C. Ronda, M. Galià, V. Cádiz, *Polym. Degrad. Stab.* **2010**, *95*, 1269.
- [25] M. M. S. Hirschler, S., in *Flame Retardants 92*, Elsevier Applied Science, London/New York, 199277.
- [26] R. Bacaloglu, U. Stewen, *J. Vinyl Addit. Technol.* **2001**, *7*, 149.
- [27] H. Zhu, W. Wang, T. Liu, *J. Appl. Polym. Sci.* **2011**, *122*, 273.